# Harmonics on the Electromagnetic Torque of a Slip Energy Recovery System with Two Thyristor Bridges and no DC Coil

M. T. Outeiro [1], E. S. Saraiva [2]

[1] Instituto Superior de Engenharia de Coimbra,
Rua Pedro Nunes - Quinta da Nora
3030-199 Coimbra (Portugal)
Telef.:+351 239 790200 fax:+351 239 790201 e-mail: touteiro@isec.pt

[2] Faculdade de Ciências e Tecnologia, University of Coimbra,
Universidade de Coimbra - Polo II,.
3030-290 Coimbra (Portugal)
Telef.: + 351 239 79 62 00, fax: + 351 239 79 62 47 e-mail: esaraiva@deec.uc.pt

**Abstract***:* This paper presents the study of the electromagnetic torque harmonic distortion of a slip energy recovery system (SERS), whose converter is constituted by two thyristor bridges and no DC coil. A brief explanation of the circuit configuration will be made. To perform the harmonic study, a special Matlab code program was developed, with several special features.
The influence of power electronic converters on the electromagnetic torque is analyzed and its oscillations are explained by considering the interaction between the stator and the rotor fundamental and harmonic currents.

***Index Terms*--** Harmonic analysis, slip energy recovery system, converter control strategy, Matlab/Simulink.

## 1. Introduction

The method of motor speed control which increases efficiency by returning the slip power, back to the system, is known as slip energy recovery system.

However, this system presents some inconveniences, for example, the low power factor, extra losses, the harmonic current generation and the electromagnetic torque oscillation. As a consequence, electromechanical vibrations are generated, which can cause motor failure, and therefore, a need for motor rewinding and/or substitution.

As it is well known, power electronic converters are generators of harmonics, both on the mains side and on the motor side, and these harmonics are transferred from one side to the other. In a slip energy recovery system (SERS), harmonics are produced and exist, not only on the rectifier side, but also on the inverter side and on the motor through the DC link. These harmonics will cause some problems on the functionality of the system and are also sent into the network. Therefore, they have been object of study by several investigators.

R. Hanna [1] presented some techniques of reduction of the harmonic content produced by adjustable speed drives. After a brief presentation of the main harmonic sources, the need to comply with harmonic standard IEEE 519 – 1982 is demonstrated. The effects of harmonics on static devices and on electrical machines are examined. Methods of reducing them and installation examples are presented.

Y. Baghzouz [2] introduced a method to evaluate the harmonic currents and voltages associated with the slip power recovery drives. The harmonic components are determined from closed form expressions that are functions of the numerical values of the distorted waveforms. The non-periodic nature of the stator currents and the existence of harmonics in the rotor currents and voltages for several speeds of operation are presented.

L.Refoufi and P. Pillay, [3] analyzed the impact on the power system of a slip energy recovery induction motor drive system in terms of harmonic generation. A hybrid dq/abc model to predict key waveforms of a chopper-controlled slip energy recovery induction motor drive (SERIMD) was used. They studied in detail the waveforms of the supply, stator and inverter currents, for a wide operation range. They concluded that this drive generates subharmonics of the supply frequency which could possibly cause flicker in the electrical systems. The phase of the subharmonics is shown to be important with different supply phases experiencing different time domain waveforms, even with the same harmonic content.

W. Zakaria and al [4] proposed a model of machine that has a double–circuit in the rotor, one is delta connected and the other is star connected, these two windings feeding a 12-pulse diode bridge rectifier, in

order to reduce the time harmonics in the machine. The main feature of the proposed system is the significant reduction of the harmonics of the rotor flux linkage, who leads to a significant reduction in the stator current harmonics and consequently the pulsating components of the electromagnetic torque are also reduced significantly, with the proposed system.

A. Dell'Aquila and al [5] developed a method for the analysis of the line-side harmonic currents produced by a variable speed induction motor drive. The proposed method permits the calculation of the distorted current waveforms, injected by the drive system into the grid. Simulation results are compared with the experimental harmonic distortion generated by a variable speed drive.

G. Marques and P. Verdelho [6] presented a circuit configuration that includes a boost-chopper that connected the diode rectifier bridge to the dc-link voltage, which is generated by a capacitor and a voltage-source inverter (VSI). To solve the drawbacks caused by the harmonics introduced by the rotor rectifier they presented two different solutions. The first solution introduces additional inductances connected to the ac side of the rotor circuit and the second solution compensates the stator current harmonics by a PWM-VSI that can work simultaneously as an inverter and as an active power filter.

J. Faiz and al [7] studied the harmonics and performance improvement of a slip energy recovery induction motor drive, based on the hybrid model dqabc. The sinusoidal pulse-with modulation (SPWM) control technique is used to improve the power factor of the drive and to weaken the low order harmonics injected into the supply. With the PWM technique, self-commutated switches (GTO or IGBT) replace the inverter thyristors and the inverter may operate with a zero reactive power.

N. Hoshi and al [8] presented a study of a slip power recovery system having sinusoidal rotor currents. The proposed system uses a PWM boost rectifier as a substitute for a diode rectifier and a boost chopper in a conventional compact-type slip-power recovery system. The system proposed, solves the problem of the distorted stator and rotor currents as the rotor currents become sinusoidal waves.

As can be observed thorough these studies, power electronics applied to industrial power systems, particularly this kind of system, has gone thorough enormous technological advancements during the last years. Associated to these advances in the power electronic, the problem of the harmonics has continued deserved the interest of the investigators, as shown through these studies.

This paper presents a interaction between the fundamental and the harmonics of stator and rotor currents, on the harmonics present on the electromagnetic torque.

The novelty of the present study is the fact that the system configuration does not have the DC link coil in the intermediate circuit.

## 2. Circuit configuration

Fig.1 shows the circuit configuration of the SERS used in this study, with particular emphasis on the control system, represented by the S1 and S2 subtractors and NR and IR, regulators. Besides the control system, this circuit is composed by: 1) three-phase feedback transformer, represented by the Dd0 box; 2) asynchronous motor M, fed through the stator by the three-phase mains RST; 3) the rotor windings, which are connected to the thyristor bridge SR1; 4) SR1 and SR2, which are the 6-pulse, 3-phase thyristor bridge rectifier and the 3-phase thyristor bridge inverter, respectively; 5) system components TG, IM and UM, which are used to measure the speed, current and voltage, necessary to the system control.

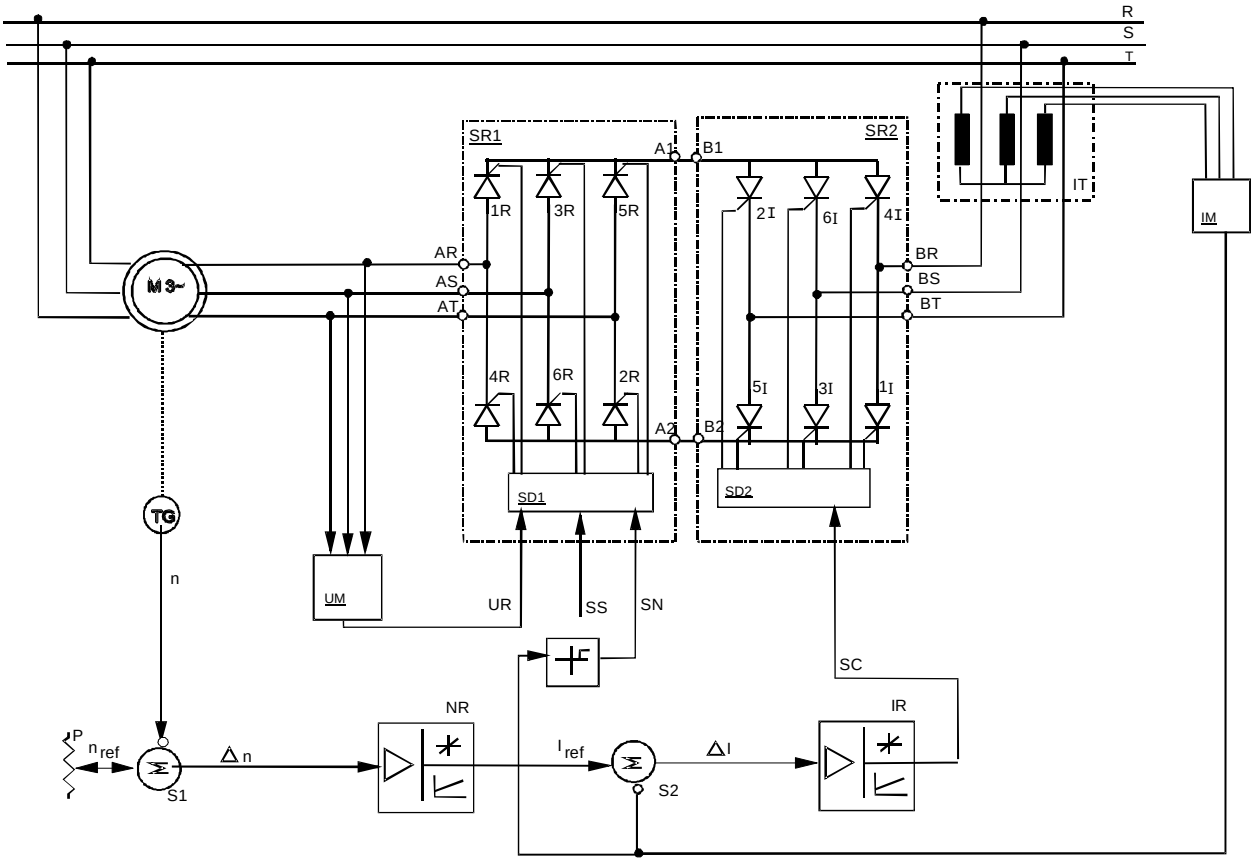


Fig. 1 Circuit configuration of the slip energy recovery system.

## 3. Electromagnetic and mechanical load torque equations

The electromagnetic torque was measured directly from the block model of the three-phase asynchronous machine selected on the Power System Blockset (PSB) library of Matlab/Simulink software. It was chosen to enter the parameters in S.I. units. All electrical variables and parameters are referred from the stator. All stator and rotor quantities are observed in the rotor reference frame (qd frame). Considering an electrical system with these conditions, the electromagnetic torque is given by the equation (1).

$$T_e = 1.5p\left(\varphi_{ds} i_{qs} - \varphi_{qs} i_{ds}\right) \qquad (1)$$

where; p is the number of pole pairs, $\varphi_{ds}$ and $\varphi_{qs}$ are the stator d and q axis fluxes respectively and $i_{ds}$ and $i_{qs}$ are the d and q axis stator currents respectively.

The mechanical load torque was implemented by Simulink blocks. The determination of this characteristic, took into account the information supplied by the manufacturer, namely: moment of inertia (J) = 142.50 kg.m$^2$, rated speed ($N_N$) = 985 r.p.m, rated torque ($T_N$) = 1405 kg.m.

The information supplied by the manufacturer was transformed into S.I. units and a curve-fitting led to the equation (2), where $w_m$ is the mechanical speed:

$$T_{load} = 206{,}745 - 1{,}50325 \times 3 \times wm + \\ + 0{,}146636 \times (3 \times wm)^2 + \\ + 1447{,}22 \times e^{-\left(\frac{3 \times wm}{11{,}75}\right)} \qquad (2)$$

This equation is only valid for positive speed.

## 4. Analysis of the electromagnetic and load torque plots

Fig. 2 shows the electromagnetic and mechanical load torques obtained from the model developed in Matlab/Simulink of the circuit of Fig. 1.

During rheostatic starting, the torque oscillates between 11.8 x10$^4$ N.m and -3x10$^4$N.m with decaying oscillations, which is the normal starting behaviour.

At about 4.7s the currents start flowing through the bridge converters and the electromagnetic torque tends to a steady state oscillating behaviour, with a maximum of 1.8x10$^4$ N.m and minimum of 0.4x10$^4$ Nm. This corresponds to an alternating/average value of (1.8-0.4)/(1.8+0.4)=0.64 for the steady state, which is much

worse than the equivalent value when a DC link coil is used.

The load torque is almost constant in steady state, and corresponds to the average value of the electromagnetic torque. The peak-to-peak value of the steady-state electromagnetic torque (1.4 x $10^4$ N.m ) is much lower than the peak–to-peak value during rheostatic starting (14.8 x $10^4$ N.m ).

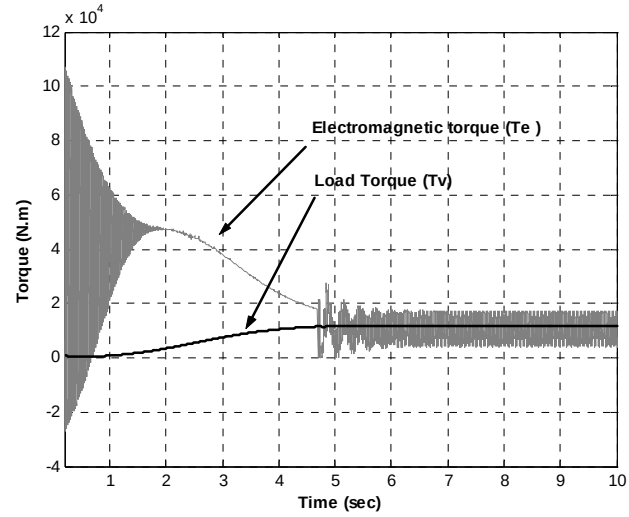


(a)

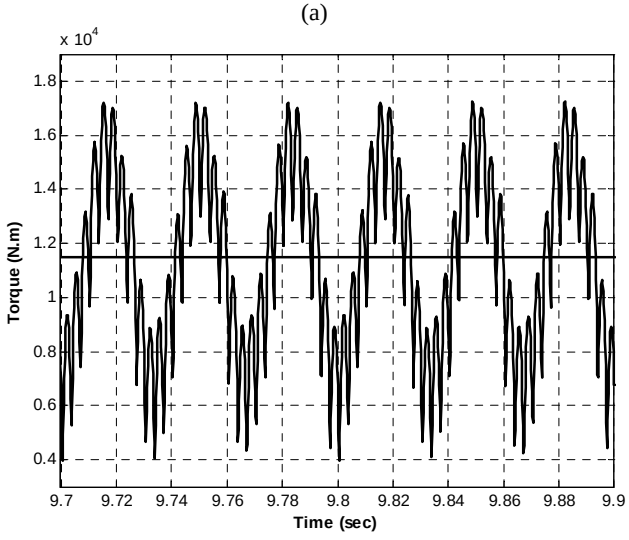


(b)

Fig. 2 Electromagnetic and load torques plots.

## 5. Harmonic analysis

To perform the harmonic study a special Matlab code program was developed, with several special features, namely, the possibility to observe a large frequency range (frequencies until 2500Hz can be observed) and high plot resolution. The obtained results for stator and rotor currents and for the electromagnetic torque are shown on Fig. 3 to Fig 5. These figures show the signal amplitude versus frequency modulus. In order to take the maximum information concerning the spectrum of the variable, a logarithmic y-axis scale is adopted.

The Discrete Fourier Transform (DFT) was used in this study and its moduli coefficients $a_0$, ak and $b_K$ were calculated. A total of 10000 samples was used for the calculations.

### *A. Rotor current, $I_r$*

The harmonic components of the rotor currents due to the six-pulse rectifier converter (SR1), due to the DC side average value, appears at frequencies given by equation (3), with k=0, 1, 2, 3

$$f^{R}_{r,h} = |1 \pm 6k|\, s f_{ms} \qquad (3)$$

From equation (3), when k=0 and s=0.1 the fundamental rotor frequency will be equal to 5Hz. The 5th, 7th, 11th, and 13th harmonic orders are also present in the rotor current and according to equation (3) they will be equal to 25Hz, 35Hz, 55Hz and 65Hz, respectively.

As can be observed by the rotor current spectrum shown in Fig. 3a, Fig. 3b and Table I, the rotor current frequencies reflects the DC current frequencies with two side-bands of the fundamental rotor frequency which is 5Hz. Harmonic components due to the six-pulse inverter that appear on the DC current at frequencies multiples of 300Hz, appear in the rotor currents with two side-bands of m300Hz±5Hz, which for m=1 will corresponds to frequencies of 295Hz and 305Hz.

The DC current distortion introduced by the six-pulse inverter is also reflected on the rotor currents, however, resulting in the appearance of additional harmonics, given by equation (4), with k,m=0, 1, 2, 3,…

$$f_{r,h} = |1 \pm 6k|\, s f_{ms} \pm 6m f_{ms} = \left(|1 \pm 6k|\, s \pm 6m\right) f_{ms}, \qquad (4)$$

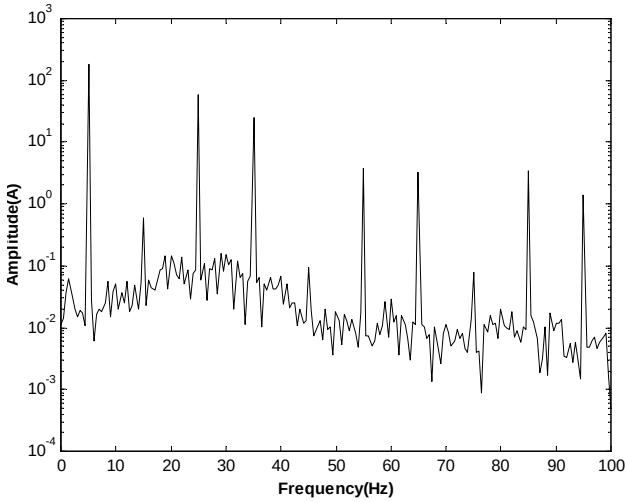


(a)

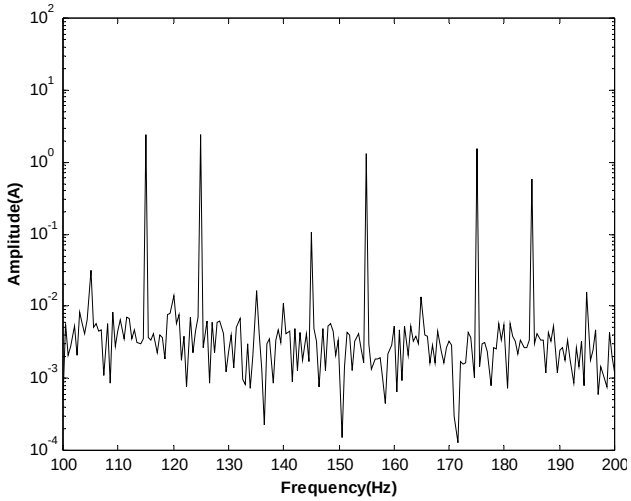


(b)

Fig.3 - Frequency spectra of the rotor current for slip=0.1

Table I - Frequencies and amplitudes of the rotor current in phase a, for slip=0.1.

| Frequency Modulus (Hz) | Amplitude (A) |
|---|---|
| 5 | 185 |
| 25 | 59.7 |
| 35 | 25 |
| 55 | 4 |
| 65 | 3 |
| 85 | 3.5 |
| 95 | 1.5 |
| 295 | 16.2 |
| 305 | 14.8 |

*B. Stator current, $I_s$*

A DC component of the rotor current, establish a rotating magnetic field in the air gap and induced voltages in the stator winding at frequency given by equation (5),

$$f_m = (1-s)\, f_{ms} \qquad (5)$$

where s is the slip and $f_{ms}$ is the fundamental frequency. For s=0.1 and $f_{ms}$=50Hz, this corresponds to a 45Hz with positive sequence.

Similarly a rotor current frequency $f_r$, manifests itself in the stator current frequencies of ($f_r$+$f_m$) with $f_r$>0, for positive sequence rotor currents, and $f_r$<0, for negative sequence rotor currents. Adding the effect of motor speed to the rotor-current frequencies, the reflected stator frequencies are given by equation (6), with k=0,1,2,3,....

$$\begin{aligned} f_{s,h}^{R} &= \left(f_r + f_m\right) = \\ &= (1 \pm 6k)sf_{ms} + (1-s)f_{ms} = \\ &= (1 \pm 6ks) f_{ms} \end{aligned} \qquad (6)$$

Adding the effect of rotor side-band frequencies due to the inverter harmonics, the frequencies of the induced harmonics present in the stator, considering these two effects are given by equation (7), with k,m=0, 1, 2, 3.

$$f_{s,h} = (1 \pm 6ks \pm 6m)\, f_{ms}, \qquad (7)$$

This equation will be reduced to equation (6) for m = 0.

Fig. 4a and Fig. 4b show the stator current spectrum and Table II the corresponding frequencies moduli and amplitudes. Using equation (6), if s=0.1 and k=0, the fundamental frequency, will be equal to 50Hz.

Using equation (7), if k=1 and m=0, the 5th and 7th harmonics orders of the rotor current appear in the stator at frequencies moduli of |-25 +45|=20Hz and |+35 +45| = 80Hz, If k=2 and m=0, the 11th and 13th harmonics of the rotor current appears in the stator at frequencies of moduli |-55 +45|=10Hz and |65 +45|=110Hz. If k=0 and m≠0, equation (6) gives the effects of frequencies due to the inverter harmonics. The 300Hz inverter referred to the stator introduces side-band frequencies moduli $|\pm 300 + 45 \pm 5|$: of 250Hz, 260Hz, 340Hz and 350Hz. The large peaks of stator frequency moduli of 250Hz and 350Hz correspond to the rotor frequencies of 295Hz and 305Hz, respectively. If k=1 and m=1, the frequencies moduli of 220Hz, 380Hz and 280Hz, 320Hz will appear.

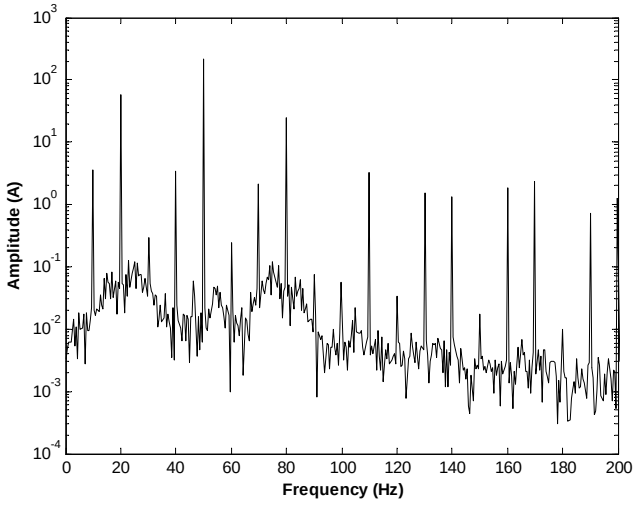


(a)

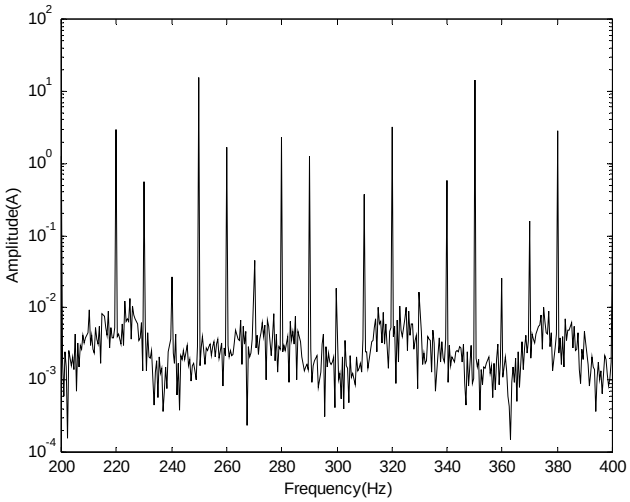


(b)

Fig.4 - Frequency spectra of the stator current for slip=0.1.

Table II- Frequencies and amplitudes of the stator current in phase A for slip=0.1.

| Frequency Modulus (Hz) | Amplitude (A) |
|---|---|
| 10 | 3.8 |
| 20 | 57.5 |
| 50 | 221 |
| 80 | 24.5 |
| 110 | 3.2 |
| 220 | 1.6 |
| 250 | 15.7 |
| 280 | 2.2 |
| 320 | 3.2 |
| 350 | 14.3 |
| 380 | 3 |

### *C. Electromagnetic Torque, $T_e$*

Fig.5a and Fig. 5b show the harmonics of the electromagnetic torque, which can be explained by the interaction of the magnetomotive force waves set up by the stator and the rotor fundamental and harmonics. The electromagnetic torque can be calculated using equation 8 obtained from [9], in the stator reference frame.

$$\Gamma_{em} = \frac{3}{2} \times p \times L_{sr} \left( i_{qs} i_{dr} - i_{ds} i_{qr} \right) \qquad (8)$$

The spectrum of the electromagnetic torque component due to the interaction between a sinusoidal stator current component and a sinusoidal rotor current component can be obtained as follows:

$$\Gamma_{em} = k \times \left( \cos\left( w_s \right) t \right) \times \left( \cos\left( w_r + w_m \right) t \right) \qquad (9)$$

$$= \frac{k1}{2} \times \left[ \cos\left( f_s - fr - fm \right) t - \varphi + \cos\left( f_s + fr + fm \right) t + \varphi \right]$$

where, k and k1 constants, $w_s$ the angular speed of the stator currents; $w_r$ the angular speed of the rotor currents, $w_m$ the mechanical speed in radelec/s , $f_s$ the stator current frequency; $f_r$ the rotor current frequency and $f_m=(1-s).f_s$ the mechanical frequency in electrical Hertz.

The values of $w_s$ and $w_r$ can be positive or negative depending on the positive or negative characteristics of the sequence.

As shown in Fig. 5a and Fig. 5b, the most relevant peaks of the electromagnetic torque spectrum appear at frequencies multiples of 30Hz.

The Table III lists the ones that correspond to a value higher than 12N.m.

The Table IV shows the most significant combined frequencies of the stator and the rotor currents. When equation 9 is applied, the most relevant frequencies that appear in electromagnetic torque are obtained.

The continuous component (0Hz) is equal to 11504N.m and is mainly a consequence of the interaction between the fundamental frequency of the stator 50Hz and the fundamental frequency of the rotor 5Hz (100%). The interaction of the +80Hz frequency of the stator and the +35Hz of the rotor (14.98%), -250Hz of the stator and -295Hz of rotor (0.62%) and +350Hz of the stator and +305Hz of rotor (0.51%). The 30Hz frequency of the torque corresponds to 4213.9N.m and is mainly a consequence of the interaction between the fundamental frequency of the stator +50Hz and +35Hz of the rotor (13.5%), the interaction of the -20Hz frequency of the stator and the +5Hz of the rotor (26%), the +80Hz of the stator and the -25Hz of rotor (11.8%) and +80Hz of the stator and the +65Hz of rotor (0.22%). The frequencies of 60Hz, 90Hz, 240Hz, 270Hz, 300Hz, 330Hz, 360Hz, 600Hz, in the electromagnetic torque spectrum, result from the interaction of some rotor and stator frequencies of different orders.

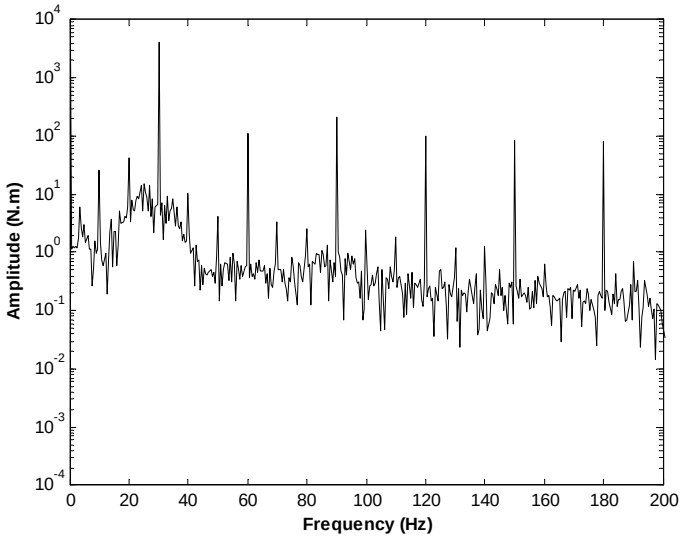


(a)

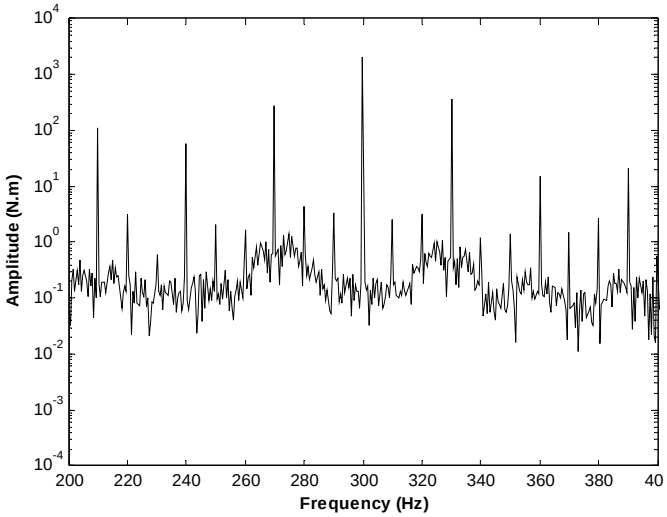


(b)

Fig.5 - Frequency spectra of the electromagnetic torque for slip=0.1.

Table III - Frequencies and amplitudes of electromagnetic torque

| Frequency Modulus (Hz) | Amplitude (N.m) | % Amplitude of DC Component |
|---|---|---|
| 0 | 11504 | 100 |
| 30 | 4213.9 | 36.62 |
| 60 | 108.5 | 0.94 |
| 90 | 215 | 1.86 |
| 120 | 100 | 0.86 |
| 150 | 85.2 | 0.74 |
| 180 | 82 | 0.71 |
| 210 | 105 | 0.91 |
| 240 | 60 | 0.52 |
| 270 | 279.6 | 2.43 |
| 300 | 2000 | 17.38 |
| 330 | 354.8 | 3.08 |
| 360 | 15 | 0.11 |
| 390 | 20 | 0.17 |
| 510 | 22 | 0.19 |
| 540 | 20 | 0.17 |
| 570 | 145 | 1.26 |
| 600 | 444 | 3.85 |
| 630 | 167 | 1.45 |

## 6. Conclusions

This paper presents the study of the influence of power electronic converters of a slip energy recovery system (SERS) on the electromagnetic torque. A brief explanation of the circuit configuration was made, and to perform the harmonic study, a special Matlab code program was developed, with several special features.
The electromagnetic torque harmonic distortion is analyzed and its oscillations are explained by considering the interaction between the stator and the rotor fundamental and harmonic currents. The simulation results show a strong disturbance in the electromagnetic torque in the steady state and the corresponding spectrum.

## References

[1] R. Hanna, "Harmonics and technical barriers in adjustable speed drives"., IEEE Trans. on Industry Application, vol. 25, Nº5, Sept.1989

[2] Y. Baghzouz,, "Harmonic analysis of slip-power recovery drives"., IEEE Trans. on Industry Application, vol. 28, Nº1, Jan./Fev..1992.

[3] L. Refoufi and P. Pillay, "Harmonic analysis of energy recovery induction motor drives," IEEE Trans. on Energy Conversion, vol.9, Dec.1994.

[4] W. Zakaria, S. Alwash and A. Shaltout, "A novel double-circuit-rotor balanced induction motor for improved slip-energy recovery drive performance," Part I - Modeling and Simulation, IEEE Trans. on Energy Conversion, pp. 563-569, Sept.1996.

[5] A. Dell'Aquila, A. Lassandro and P. Zanchetta, "Modeling of line side harmonic currents produced by variable speed induction motor drives"., IEEE Trans. on Energy Conversion, vol. 13, Nº3, Sept.1997.

[6] G.D. Marques and P. Verdelho, “A simple slip-power recovery system with a DC voltage intermediate circuit and reduced harmonics on the mains”. IEEE Trans. on Industrial Electronics. Vol.47, pp 123-132, February 2000.

[7] J. Faiz, H. Batari and E. Akpinar, “Harmonic analysis and performance improvement of slip energy recovery induction motor drives”. IEEE Trans. Power Electronics, vol 16, pp. 410-417, May 2001.

[8] N. Hoshi and al “A compact type slip-power recovery system with sinusoidal rotor current for large pump/fan drives”. IEEE Trans. Power Electronics, vol 16, pp. 410-417, May 2001.

[9] J. Chatelein, Machines Électriques Tome 1, Dunod (1983), pp.240.

TABLE III- Frequencies that appears in the electromagnetic torque for slip=0.1

| Frequency (Hz) | | Frequencies (Hz) | Amplitude of rotor x stator ($A^2$) | % of fundamental rotor x stator | Relevant frequency in torque (Hz) |
|---|---|---|---|---|---|
| Stator | Rotor | | | | |
| 50 | 5 | 0<br>100 | 221x185 | 100 | 0 |
| | -25 | -20<br>+70 | 221x59.7 | 32.2 | - |
| | +35 | -30<br>+130 | 221x25 | 13.5 | 30 |
| | -55 | +60<br>+40 | 221x4 | 2.16 | 60 |
| | +65 | -60<br>+160 | 221x3 | 16.2 | 60 |
| | -295 | +300<br>-200 | 221x16.2 | 8.75 | 300 |
| | +305 | -300<br>+400 | 221x14.8 | 8 | 300 |
| -20 | 5 | +30<br>-70 | 57.5x185 | 26 | 30 |
| | -25 | -90<br>+50 | 57.5x59.7 | 8.39 | 90 |
| | +35 | -100<br>+60 | 57.5x25 | 3.51 | 60 |
| | -55 | -10<br>+80 | 57.5 x4 | - | - |
| | +65 | -130<br>+90 | 57.5x3 | 0.43 | 90 |
| | -295 | +230<br>-360 | 57.5x16.2 | 2.2 | 360 |
| | +305 | -370<br>+330 | 57.5x14.8 | 2 | 330 |
| +80 | 5 | +30<br>+130 | 24.5x185 | 11.08 | 30 |
| | -25 | +60<br>+100 | 24.5x59.7 | 35.7 | 60 |
| | +35 | 0<br>+160 | 24.5x25 | 14.98 | 0 |
| | -55 | +90<br>+70 | 24.5x4 | 0.23 | 90 |
| | +65 | -30<br>+190 | 24.5x3 | 0.22 | 30 |
| | -295 | +330<br>-170 | 24.5x16.2 | 0.97 | 330 |
| | +305 | -270<br>+430 | 24.5x14.8 | 0.88 | 270 |
| -250 | 5 | -300<br>-200 | 15.7x185 | 7.2 | 300 |
| | -25 | -270<br>-230 | 15.7x59.7 | 2.29 | 270 |
| | +35 | -330<br>-170 | 15.7x25 | 0.96 | 330 |
| | -55 | -240<br>-260 | 15.7x4 | 0.15 | 240 |
| | +65 | -360<br>-140 | 15.7x3 | 0.15 | 360 |
| | -295 | 0<br>-500 | 15.7x16.2 | 0.62 | 0 |
| | +305 | -600<br>+100 | 15.7x14.8 | 0.56 | 600 |
| +350 | 5 | +300<br>+400 | 14.3x185 | 6.4 | 300 |
| | -25 | +330<br>+370 | 14.3x59.7 | 2 | 330 |
| | +35 | +340<br>+360 | 14.3x25 | 0.87 | 360 |
| | -55 | +360<br>+340 | 14.3x4 | - | 360 |
| | +65 | +240<br>+460 | 14.3x3 | - | 240 |
| | -295 | +600<br>+100 | 14.3x16.2 | 0.56 | 600 |
| | +305 | 0<br>+700 | 14.3x14.8 | 0.51 | 0 |